DOI: 10.1143/JPSJ.81.054706

Evidence of Spin-Filtering in Quantum Constrictions with Spin–Orbit Interaction

Sunwoo KIM*, Yoshiaki HASHIMOTO, Yasuhiro IYE, and Shingo KATSUMOTO

Institute for Solid State Physics, University of Tokyo, Kashiwa, Chiba 277-8581, Japan

(Received December 28, 2011; accepted March 1, 2012; published online April 20, 2012)

A new type of blockade effect — spin–orbit-induced blockade (SOIB) — has been observed in the conduction of a quantum dot (QD) made of a material with spin–orbit interaction. The blockade arises from the spin filtering effect in a quantum point contact (QPC), which is a component of the QD. Hence the appearance of the blockade itself is evidence of the spin filtering effect in the QPC. The lower bound of filtering efficiency is estimated to be above 80%.

KEYWORDS: quantum point contact, spin filter, spin–orbit interaction, quantum dot, spin blockade

1. Introduction

The generation of spin current without external magnetic field in nonmagnetic materials is the most important issue in semiconductor spintronics.[1] The combination of spin–orbit interaction (SOI) and quantum constrictions is a promising candidate for spin filtering, and a number of device schemes have been proposed.[2–4] As is well known, spin polarization can only be obtained by breaking the time-reversal symmetry. In the proposal in ref. 2, the polarization is given by the interplay between the SOI, the geometrical asymmetry of the sample, and the current flow, which essentially causes the time-reversal symmetry breaking. In ref. 3, a quantum point contact (QPC) with the SOI was considered and again, the one-way transitions between the spin–orbit hybrid states caused by the current flow were found to be the origin of the spin polarization. The directional imbalance in the electron flow is also important for the mechanism discussed in ref. 4 though a weak magnetic field is introduced to support the polarization.

In spite of the above ingenuities, no clear experimental support has been given for them. A major difficulty lies in the detection of spin polarization through such delicate filters. On the other hand, Debray *et al.* found anomalous conductance quantization to $0.5G_q$ (conductance quantum, $G_q = 2e^2/h$) in a QPC made of a material with strong SOI.[5] This is possibly due to the spin polarization, and they also gave a possible mechanism that is driven by, again, the current flow with the aid of SOI and the electron–electron interaction around the QPC.

In this article, we present the first clear observation of spin filtering with a simple QPC made of a material with SOI,[5] through the finding of a novel blockade effect in a quantum dot (QD). We here call the phenomenon spin–orbit-induced blockade (SOIB). SOIB is similar to spin blockade in that it originates from the Pauli exclusion principle,[6] though it requires only a single QD whereas the conventional spin blockade requires two QDs in series. Furthermore, SOIB gives an estimation of the lower bound of the degree of polarization. We thus show that a QPC and a QD with the SOI can function as a spin polarizer and a detector, respectively.

SOI in a two-dimensional electron system (2DES) acts on spins as an effective magnetic field. Broken spatial inversion symmetry, e.g., lattice asymmetry (Dresselhaus SOI) or asymmetric interfaces (Rashba SOI)[7] can be the origin. SOI is stronger in materials with smaller band gaps, such as InAs, InSb, and mixed crystal (In,Ga)As. The materials are often chosen as stages for the investigation of SOI in semiconductor quantum structures.

In this paper, after the description of the samples and experimental setups in §2, the reproduced result of the experiment in ref. 5 is described in §3. More spin-specific confirmation is described in §4, which begins with a description of the experimental setup followed by the identification of the spin states in a quantum dot with the Kondo effect. The description of our new finding, "spin–orbit-induced blockade", is the main content of §4. After showing the lower bound of spin-polarization efficiency, the results are summarized.

2. Experiments

Here we adopt a pseudomorphic $In_{0.1}Ga_{0.9}As$ quantum well placed next to a GaAs/AlGaAs interface, which produces a perpendicular electric field. The layered structure shown in Fig. 1(a) was grown by molecular beam epitaxy on a (001) GaAs substrate. The 2DES carrier concentration is $1.2 \times 10^{12}\,\mathrm{cm}^{-2}$, and the Hall mobility is $8.2 \times 10^4\,\mathrm{cm}^2\,\mathrm{V}^{-1}\,\mathrm{s}^{-1}$ at 4.2 K. QPCs and QDs defined by Ti/Au split gates were fabricated by electron-beam lithography. The specimens were cooled to 50 mK in a dilution fridge.

3. Conductance of Quantum Point Contact with SOI

Figure 1(b) shows the conductance of a single QPC [gate configuration in Fig. 1(a)] as a function of the split gate voltage. A clear plateau at half-conductance quantum ($0.5G_q$, 0.5 plateau) is observed and the result is similar to that presented by Debray *et al.*[5] for a QPC also with strong SOI. They explained the 0.5 plateau along spin filtering, as noted in the introduction section. No further experimental support of spin-polarized transport has been given, other than the response to magnetic field, or to asymmetry in the QPC potential.

Henceforth, we present strong experimental support of the hypothesis of spin-polarized transport on such a 0.5 plateau, regardless of the symmetry-breaking mechanism. As a first simple check, conduction under a perpendicular magnetic field of up to 10 T was examined. Above 7 T, Zeeman splitting is large enough to dominate the subband structure at the QPC and a clear $0.5G_q$ plateau appears, as shown in

*E-mail: swkim@issp.u-tokyo.ac.jp

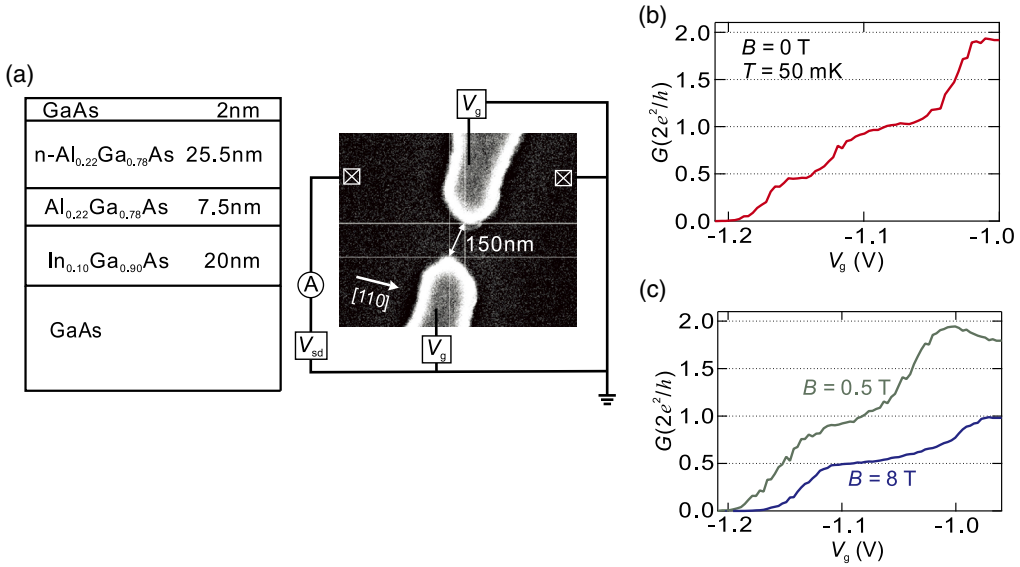

Fig. 1. (Color online) (a) Schematic cross-sectional view of layered structure grown by MBE. Nominal Si concentration in the modulation doped layer is 6×10^{18} cm^{-3}. The right figure is the electron beam micrograph of the metallic gate configuration for QPC. (b) Two wire conductances of QPC at 50 mK as a function of symmetrically applied split gate voltage. Separately measured contact resistance is subtracted. A clear $0.5G_q$ quantized plateau is observed. (c) Perpendicular magnetic field variation of the $0.5G_q$ plateau, which disappears at 0.5 T and reappears as a broad plateau around 8 T.

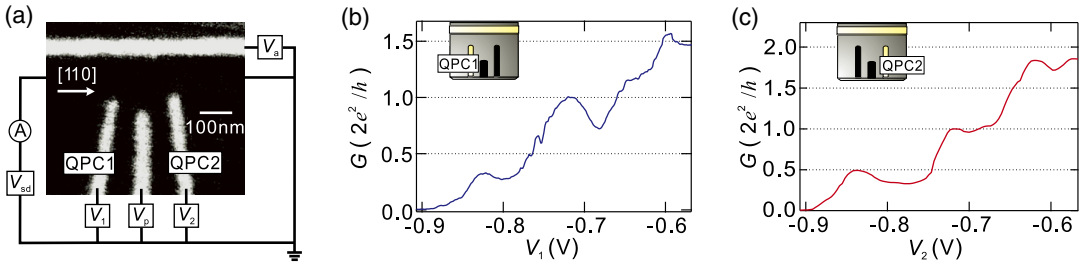

Fig. 2. (Color online) (a) Scanning electron micrograph of split gate configuration for QD. Measurement circuit is schematically drawn. (b) Conductance of QPC1 at 50 mK as a function of V_1 with $V_a = -0.7$ V and V_p, $V_2 = 0$ V. (c) Conductance–gate voltage (V_2) characteristics of QPC2 with $V_a = -0.7$ V and V_p, $V_1 = 0$ V.

Fig. 1(c), confirming that spin filtering can cause half-quantum discretization. Interestingly, the $0.5G_q$ plateau once disappears at around 0.5 T. According to ref. 5, an asymmetric confinement potential is indispensable for spin filtering, and if similar mechanism is applicable to the present case, a weak perpendicular field would reduce boundary scattering,[8] and the resultant "recovery" of symmetry would be a possible cause of the disappearance of the plateau.

4. Spin-Polarized Transport in Quantum Dot

4.1 Experimental setup

Although the above results are in agreement with the hypothesis of spin filtering in the QPC, support from more spin-specific phenomena is required in order to prove that the 0.5 plateau is indeed due to spin filtering. We hence proceed to the conduction through a QD of the same material. Through the clarification of the electronic states in the QD, it will be possible to exclude physical origins other than spin filtering. As shown in Fig. 2(a), our QD is connected to the electrodes through two QPCs (QPC1, QPC2) on both sides. As depicted in Figs. 2(b) and 2(c), these QPCs also show 0.5 plateaus at around V_1, $V_2 = -0.8$ V, though the absolute values of conductance are significantly lower than e^2/h. The deviations can be attributed to the scattering by the potential due to the surrounding gates,[9] which does not present in the sample shown in Fig. 1(a). In forming a QD, QPC1 was set on the 0.5 plateau while QPC2 was on the 1.0 plateau. Therefore, if we apply the spin-filtering hypothesis, the transport through QPC1 is spin-selective while that through QPC2 is not. The Coulomb peaks were significantly broadened, as shown in Fig. 3(a), owing to the half-opened dot condition, though we still could clearly distinguish peaks from the neighboring ones.

4.2 Kondo effect

As noted above, we should establish the spin state in the dot to examine the hypothesis. Here, we utilize the Kondo effect to obtain concrete information on the spin states.[10] The Kondo effect in conduction through QDs is characterized by an anomalous enhancement of conductance in Coulomb valleys with decreasing temperature and by zero-bias conductance peaks.[11] Because these features are the results of interaction between electron spins via localized spins in the dot, the QD should have an unpaired electron at

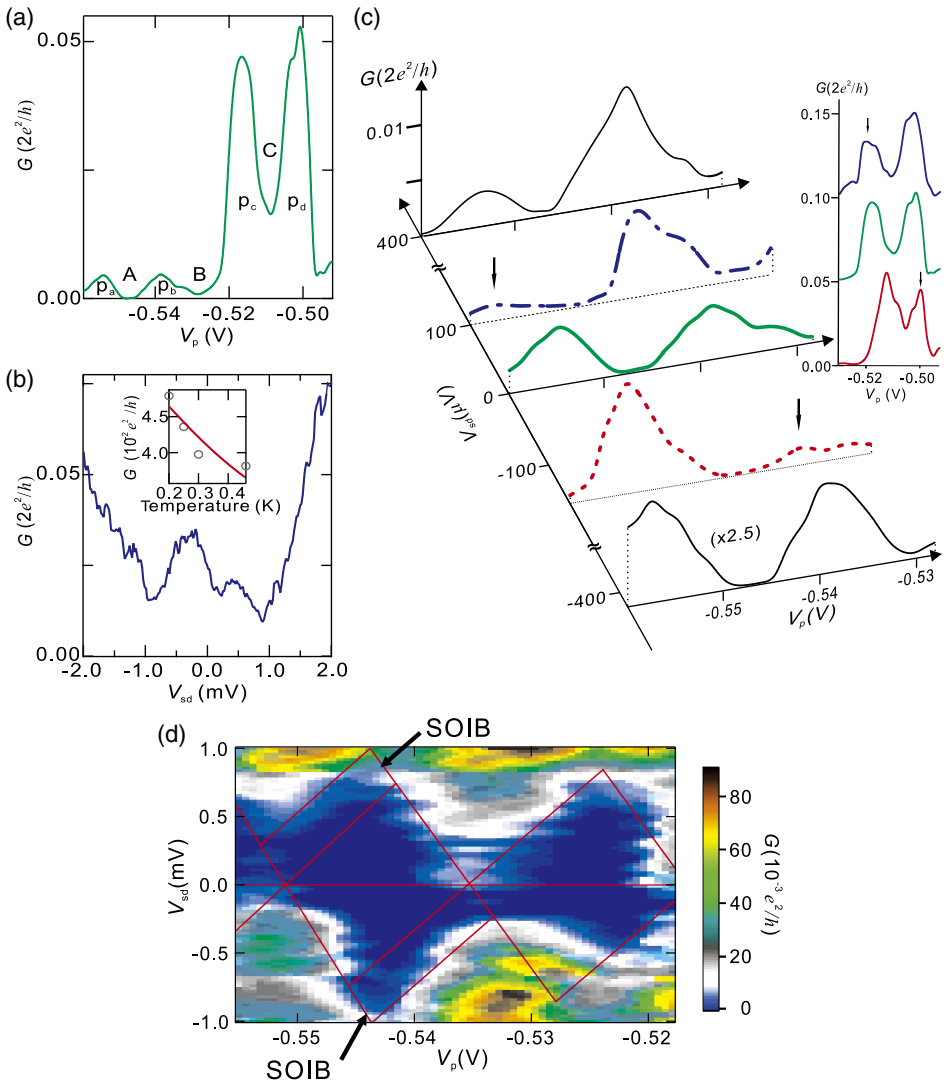

Fig. 3. (Color online) (a) QD conductance at 50 mK as a function of plunger gate voltage V_p. Four Coulomb peaks are observed. The peaks and the valleys are labeled p_a–p_d, and A–C, respectively. (b) QD conductance at 50 mK as a function of V_{sd} at the midpoint of Coulomb valley C. The inset shows the temperature dependence of finite-bias QD conductance and the line is the fitted result of the Kondo temperature dependence with T_K of 995 mK. (c) Quantum dot conductance at 50 mK as a function of plunger gate voltage V_p for five representative V_{sd} conditions. At $V_{sd} = 0$ [solid (green) curve] there are four Coulomb peaks in this range of V_p, as indicated in the figure. At $V_{sd} = 100\,\mu V$ [dotted (blue) curve], we observe that peak p_a disappears and p_c diminishes, as indicated by vertical arrows, and at $V_{sd} = -160\,\mu V$ [broken (red) curve] peak p_b disappears and p_d diminishes. Further increment of $|V_{sd}|$ recovers the double peak configuration. The inset shows similar tendencies of peaks p_c and p_d. (d) Color plot of QD conductance on V_p–V_{sd} plane around valleys A and C. The Coulomb diamonds are marked by red lines. The SOIB regions [see Fig. 4(e)] are also indicated by black arrows.

the topmost level in the valleys with the Kondo effect. We looked for such a Coulomb valley among few tens of Coulomb oscillation periods.

In Fig. 3(a), where we index Coulomb valleys from A to C and peaks from p_a to p_d, the candidate for a Coulomb–Kondo valley is C. Firstly, Coulomb peaks at both sides of C (p_c and p_d) have similar and outstanding heights, indicating that these two peaks are through the same orbital state (i.e., the Kramers degenerated state), which has large coupling constant Γ to the electrodes.[12,13] This means the Kondo temperature T_K, which can be approximated at the midpoint of the valley with the Coulomb repulsion parameter U as

$$T_K = \frac{\sqrt{\Gamma U}}{2}\exp\left[-\frac{\epsilon(\epsilon+U)}{\Gamma U}\right] = \frac{\sqrt{\Gamma U}}{2}\exp\left(-\frac{3\pi U}{4\Gamma}\right), \quad (\epsilon = -U/2), \quad (1)$$

is higher in C. Here, ϵ is the position of the Fermi energy from the chemical potential at the apex of the diamond for $V_{sd} = 0$. Secondly, the current–voltage (I–V) characteristic shows a broad double-peak structure at 50 mK, as displayed in Fig. 3(b). This is similar to the I–V curve for the Kondo effect, except for the zero-bias dip. The dip at the center is observed throughout the diamond at valley C and cannot be attributed to some interference effect. Instead, a natural interpretation is that the sharp peak of Kondo resonance, which arises from the interexchange of electrons through QPC2, is blocked in total transport by spin filtering at QPC1 as discussed later. Lastly, the enhancement of conductance with cooling is observed, as shown in the inset of Fig. 3(b). If we fit the well-known temperature dependence of conductance,[14,15] $G(T) = G_0 - G_1[T_K{}^2/(15T^2 + T_K{}^2)]^{1/4}$, for the spin $-1/2$ Kondo effect to the data, we obtain a reasonable T_K of about 1 K. From the above analysis, we can

safely say that the SU(2) (spin 1/2) Kondo effect arises at valley C.

4.3 *Spin–orbit-induced blockade*

With the knowledge of the spin state in valley C, the topmost state in valley A is identified as the one with an unpaired electron, whereas the dot must have a closed shell structure in valley B.

Our target of analysis hereafter is valley A, where the bordering peaks (p_a and p_b) are significantly lower than those of valley C, i.e., Γ is much smaller, hence, from eq. (1), T_K is very low. The Kondo effect is thus beyond the experimental scope here. We observe normal Coulomb oscillation [solid (green) curve in Fig. 3(c)] at zero-bias ($V_{sd} = 0$). At a small positive bias ($V_{sd} = 100\,\mu V$) where broadening and height growth of the Coulomb peaks are expected for increasing $|V_{sd}|$, surprisingly, peak p_a vanishes while p_b shows ordinary growth [dotted (blue) curve in Fig. 3(c)]. This is reminiscent of spin blockade in double QD systems.[6] However, in the present case, when the sign of V_{sd} is reversed to negative, peak p_b vanishes whereas p_a grows as usual [broken (red) curve in Fig. 3(c)]. These anomalous behaviors disappear and conventional Coulomb oscillation is restored when the absolute value of $|V_{sd}|$ exceeds about $250\,\mu V$ [black curves in Fig. 3(c)]. The results are summarized in Fig. 3(d).

Because p_a and p_b arise from the same orbital level, the major difference between them is the total spin in the dot. In the following we discuss that the spin selectivity (SS) at QPC1 is the origin of the unexpected antisymmetric blockade. For simplicity, we henceforth assume that only up-spin (↑) electrons can transmit through QPC1 without losing generality. The following discussion also holds if an entanglement between the direction of the electron transmission and the spin (e.g., left-↑ and right-↓) is assumed instead of the simple SS. Therefore, we cannot compare the present results with existing theoretical proposals[16,17] for such spin-selectivity in quantum constrictions with the SOI.

Let us begin with peak p_b, where the topmost orbital level is already occupied by an unpaired electron. When a positive V_{sd} is applied, the flow sequence of electric current through the QD is as follows: first an electron tunnels from the drain into the QD through QPC2, then only ↑-electrons can escape through QPC1 with ↑-SS, but another ↑-electrons can be supplied through QPC2 [Fig. 4(c)]. Hence the process forms a finite Coulomb peak. When the bias is reversed, electrons should come in through QPC1 and go out through QPC2. When QPC2 transmits a ↓-electron, the topmost level is left with an ↑-electron and the following entrance of an ↑-electron through QPC1 is blocked owing to the Pauli exclusion principle. The current is hence blocked by the ↑-SS of QPC1 [Fig. 4(d)]. Spin flips in the dot and leakage of ↑-SS of QPC1 appear as leak current. The situation is almost the same as the spin blockade (Pauli blockade) described in ref. 6 except that another dot under finite bias was utilized to fix the spin of incoming electrons in the case of spin blockade, whereas the SS due to the SOI is used in the present case.

At peak p_a for positive V_{sd}, the flow sequence is QPC2 → the lowest empty state above the closed shell → QPC1. When a ↓-electron comes into the dot it cannot escape because of the ↑-SS of QPC1. Because the tunneling probabilities are even for ↑- and ↓-electrons at QPC2, this process eventually occurs and the flow is blocked [Fig. 4(a)]. The blockade does not take place for negative V_{sd} because ↑-electrons supplied through QPC1 can escape through QPC2 [Fig. 4(b)]. This antisymmetric blockade, what we call SOIB here, deduced from the simple assumption of SS in QPC1 perfectly agrees with the observations in Fig. 3.

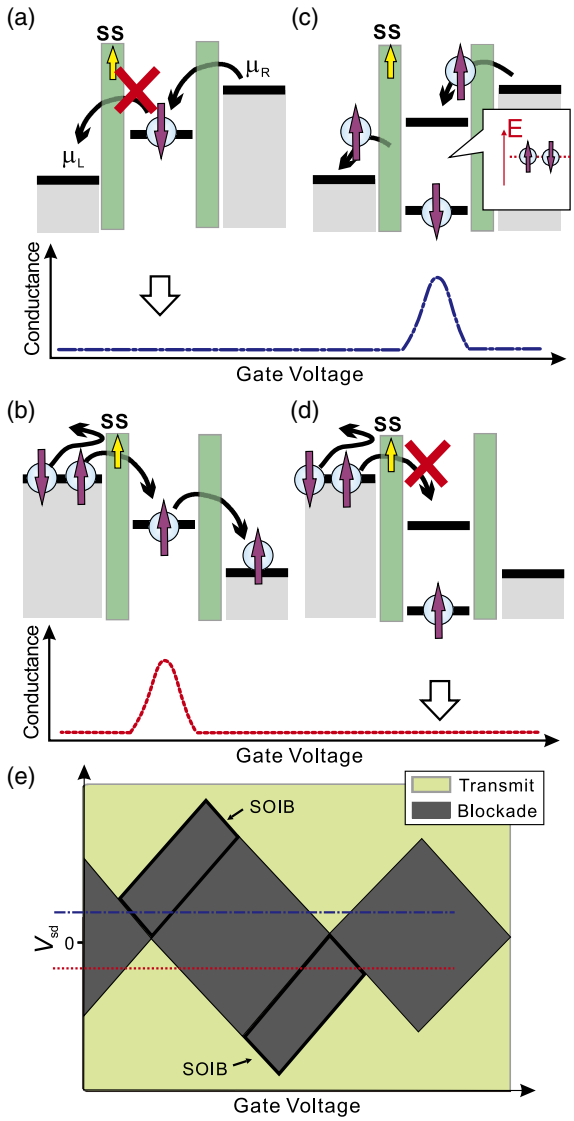

Fig. 4. (Color online) (a) At peak p_a, when a positive bias is applied, the topmost level is empty before the supply of an electron from the drain through QPC2. Sooner or later, the level is occupied by a ↓-electron, which cannot go out to the source owing to the spin selectivity in QPC1, and the current is blocked. (b) When a negative bias is applied at p_a, the electron at the topmost level can go out to the drain through QPC2 regardless of the spin direction and current flows. (c) At peak p_b, when a positive bias voltage is applied, the topmost level is already occupied with an electron before the supply of another electron with the opposite direction from the drain through QPC2. After the entrance of an electron, the level is occupied with a singlet pair and the ↑-electron can go out to the source through QPC1 with spin selectivity. (d) When a negative bias is applied at p_b, QPC1 can supply only ↑-electrons and sooner or later, a ↓-electron goes out to the drain and successive tunneling is blocked by the Pauli exclusion principle. (e) Summary of the above discussion on modified Coulomb diamond characteristics.

The SOIB can be lifted with further increase in the amplitude of V_{sd}. With increasing $|eV_{sd}|$, the energy gain from the voltage source associated with tunneling increases and when it exceeds the spacing of single-electron orbital levels, multi level transport begins forming spin bypaths or when it exceeds the gap between ↑ and ↓ channels, QPC1 is transparent for both spins. Therefore, the SOIB is lifted along a line parallel to the edge of a Coulomb diamond resulting in antisymmetric Coulomb diamonds as illustrated in Fig. 4(e).

Note that the same SOIB mechanism is in effect even in the Kondo region, though it is not so prevalent owing to the large Γ (broad level) and frequent spin fluctuation due to the Kondo effect. If we focus on the Coulomb peak heights, the same tendency as those of peaks p_a and p_b is observed for p_c and p_d [blue and red curves in Fig. 3(c)]. Peak splitting such as that of the Kondo peak in the I–V characteristics in Fig. 3(b) can be interpreted along the same lines. At zero bias, the Kondo enhancement of cotunneling is only available for QPC2 because T_K for cotunneling over QPC1 is reduced, in the sense of eq. (1), by $\exp(-3\pi eV_{th}/4\Gamma)$, where V_{th} is the SOIB-lifting threshold in V_{sd}. With increasing $|V_{sd}|$, this reduction is suppressed and the conventional conductance enhancement of the Kondo effect is restored. As a result, a broad double peak structure appears in Fig. 3(b). All the above deductions are summarized in Fig. 4(e). SOIB gives elongations of the Coulomb diamond with finite total spin in the dot. We find every characteristic point is in good agreement with Figs. 3(a)–3(d), though Fig. 3(d) has some significant distortion due to the instability of In-contained quantum dots.

4.4 Spin-polarization efficiency

So far, we have proven that spin filtering is realized in QPCs with the SOI on 0.5 plateaus and that it can be detected through the appearance of SOIB in the conduction of QDs. The asymmetry in the peak heights of p_a and p_b for finite biases [curves (2) and (3) in Fig. 3(c)] represents the ratio of reduction in the dot conductance owing to the SOIB. If we naively ignore spin fluctuation in the QD, the ratio of the residual peak conductance to the neighboring full peak height gives the nonpolarized portion in the current (note that peaks p_a and p_b utilize the same orbital state and almost the same height for each is expected without the SOIB). Therefore the "switching" ratios give the lower bound of spin-filtering efficiency in QPC1, and should be above 80% in Fig. 3.

It may be surprising that such high efficiency is obtained even with such a small In content (10%). A possible reason is the high 2DES concentration, which makes the gap between opposite spins at the Fermi circle (i.e., for fixed momentum) very large. Actually, we do not observe quantization in 2DES of the same material with much lower concentration. The enhancement of concentration decreases the effect of semiclassical electron–electron interaction adopted as the mechanism of spin polarization in ref. 5. In an actual system, if the proposed mechanism is in effect, the optimized condition would be realized when these two conflicting requests are balanced.

We would like to stress that the present scheme for spin-filtered polarization detection is widely applicable to various problems (e.g., to the 0.7 problem) regardless of the spin-polarization mechanism. On the other hand, to investigate the mechanism of polarization itself, one must combine some other devices and methods. In the present case, we believe there should be some kind of "effective magnetic field" generated by the SOI, surrounding reflecting electron channels, bias voltage, etc. on the residual conductance channel. Also, the mechanism should be clarified by, for example, adding QPCs for controlling reflecting channels or observing the response to external microwaves.

5. Summary

We have confirmed conductance quantization by the half-conductance quantum in QPCs made of $In_{0.1}Ga_{0.9}As$ 2DES. We have found that a QD, which consists of two such QPCs, shows characteristic conductance blockade (SOIB), which arises from spin-selective tunneling due to the SOI. The first observation of the SOIB directly is evidence of very high spin-filtering efficiency at QPCs with the SOI. In other words, QPCs with the SOI can function as spin polarizers and QDs as detectors.

Acknowledgment

This work is supported by a Grant-in-Aid for Scientific Research and Special Coordination Funds for Promoting Science and Technology.

1) *Semiconductor Spintronics and Quantum Computation*, ed. D. D. Awschalom, N. Samarth, and D. Loss (Springer, Heidelberg, 2002).
2) M. Yamamoto, T. Ohtsuki, and B. Kramer: Phys. Rev. B **72** (2005) 115321.
3) M. Eto, T. Hayashi, and Y. Kurotani: J. Phys. Soc. Jpn. **74** (2005) 1934.
4) A. Aharony, O. Entin-Wohlman, Y. Tokura, and S. Katsumoto: Phys. Rev. B **78** (2008) 125328.
5) P. Debray, S. M. S. Rahman, J. Wan, R. S. Newrock, M. Cahay, A. T. Ngo, S. E. Ulloa, S. T. Herbert, M. Muhammad, and M. Johnson: Nat. Nanotechnol. **4** (2009) 759.
6) K. Ono, D. G. Austing, Y. Tokura, and S. Tarucha: Science **297** (2002) 1313.
7) R. Winkler: *Spin–Orbit Coupling Effects in Two-Dimensional Electron and Hole Systems* (Springer, Berlin, 2003).
8) H. Akera and T. Ando: Phys. Rev. B **43** (1991) 11676.
9) A. Yacoby and Y. Imry: Phys. Rev. B **41** (1990) 5341.
10) L. P. Kouwenhoven and L. I. Glazman: Phys. World **14** (2001) 33.
11) W. G. Van der Wiel, S. D. Franceschi, T. Fujisawa, J. M. Elzerman, S. Tarucha, and L. P. Kouwenhoven: Science **289** (2000) 2105.
12) P. G. Silvestrov and Y. Imry: Phys. Rev. Lett. **85** (2000) 2565.
13) H. Aikawa, K. Kobayashi, A. Sano, S. Katsumoto, and Y. Iye: J. Phys. Soc. Jpn. **73** (2004) 3235.
14) T. A. Costi, A. C. Hewson, and V. Zlatic: J. Phys.: Condens. Matter **6** (1994) 2519.
15) D. Goldhaber-Gordon, J. Göres, M. A. Kastner, H. Shtrikman, D. Mahalu, and U. Meirav: Phys. Rev. Lett. **81** (1998) 5225.
16) J. Wan, M. Cahay, P. Debray, and R. Newrock: Phys. Rev. B **80** (2009) 155440.
17) O. Entin-Wohlman, A. Aharony, Y. Tokura, and Y. Avishai: Phys. Rev. B **81** (2010) 075439.